Methodologic Assessment of Beamforming Techniques for Interference Mitigation on GNSS Handheld Devices

Guillem Foreman-Campins, Lucía Pallarés-Rodríguez, Sergi Locubiche-Serra,
Gonzalo Seco-Granados, José A. López-Salcedo
Signal Processing for Communications and Navigation (SPCOMNAV)
Department of Telecommunication and Systems Engineering
Universitat Autònoma de Barcelona (UAB), IEEC-CERES, Barcelona, Spain

***Abstract*—This paper proposes a methodologic approach for the performance assessment of beamforming techniques for interference mitigation on GNSS receivers. While the use of spatial diversity has been studied extensively for antenna arrays with a high number of elements, few studies consider the case of a small antenna array that could fit into a handheld device. Some uncertainties arise from this problem, such as the optimal position of the antennas given the low space available, the strong dependance of the performance to the Direction-of-Arrival (DoA) of both the desired signal and the interference/s, the minimisation of complexity due to the power constraints in handheld devices and the optimal beamforming technique to apply in such a device. These problems are tackled in this paper, providing insight on the performance that can be expected. Specifically, this paper focuses on the performance for GNSS receivers. A complete analysis on the key performance indicators for GNSS is performed, focusing on the effective C/N_0 and phase and code jitters that can be expected after beamforming, which give a better assessment than simply taking into account indicators such as the interference null depth.**

***Index Terms*—Array processing, Beamforming, Handheld, Interference mitigation, Spatial filtering**

I. Introduction

The use of handheld devices has become massively extensive in the last years, with wireless communications and navigation applications experiencing a massive proliferation in urban environments thanks to the increasing widespread deployment of enabling technologies such as 5G, the Internet-of-Things (IoT) and Global Navigation Satellite Systems (GNSS). This has unveiled the need to cope with signal propagation impairments such as interference, multipath and spoofing that abound in such urban environments [1], [2]. With the proliferation of interference sources, jamming has become a greater concern in these environments. Two kinds of interferences are considered: unintentional and intentional. The fomer are not intended to interfere, but nevertheless cause problems in the User Equipment (UE), which include man-made interferences as well as natural phenomena. Meanwhile, intentional interferences are designed to specifically harm the user and thus pose a more significant threat.

The number of present interferences strongly depends on the location of the UE, as does its variety. In general, sites with the most human activity and traffic are more affected by interference (both intentionally and unintentionally), whereas remote sites have fewer events, although there is a high variation in activity depending on the infrastructure, the local environment and the country [3]. Most interferences have a negligible impact on the UE but, nonetheless, due to their high occurrence in the urban environment, the noticeable ones will be frequent. This leaves a great necessity to deal with these interferences in urban environments.

The use of array processing techniques, also known as spatial filtering or digital beamforming (DBF), is known to be the most powerful approach to combat the above impairments [4]. The goal is to steer the array beam toward the line-of-sight signal (LOSS) for signal-to-noise ratio (SNR) maximization, and to place nulls at the Direction-of-Arrival (DoA) of the undesired signals. Some examples of conventional beamformers are the phased array, the Capon [5] and the linear minimum mean square error (LMMSE) [6] techniques. One method that has gained traction in the past years is the Power Inversion (PI) [7], which does not take the Direction-of-Arrival (DoA) information of the LOSS (unlike Capon) and still guarantees interference mitigation despite its low implementation complexity.

Difficulties arise, though, when moving to the arena of handheld devices such as tablets or smartphones, which are driven by constraints on miniaturization, low power consumption and low-cost components. The advent of 5G cellular networks has definitely paved the way for the deployment of antenna arrays in such devices as a de-facto standard in the context of multiple-input, multiple-output (MIMO) systems [8]–[11]. This is motivated by the use of millimeter-wave signals allowing the implementation of arrays in an area with tiny dimensions. Some examples can be found in [12]–[14] for 5G applications. However, this is not the case for other technologies such as GNSS, where the antenna separation

This work has been supported in part by the Spanish Agency of Research (AEI) under the Research and Development projects PID2020-118984GB-I00/AEI/10.13039/501100011033 and PDC2021-121362-I00/AEI/10.13039/501100011033.

979-8-3503-2308-5/23/$31.00 ©2023 IEEE

(i.e. related to half the signal wavelength) is, and will still be in the mid-term, on the order of a decimeter. This poses a serious concern to the practical use of spatial filtering in these devices. However, while extensive research on antenna arrays has been done for professional GNSS receivers [15], [16], where external arrays with many antennas are typically used, the case of mass-market handheld GNSS receivers, which just allow a small number of embedded antennas, has received, to the best of our knowledge, very little attention.

Hence, the objective of this paper is to explore the feasability of performing robust interference mitigation in handheld GNSS devices with a small number of antenna elements. Additionaly, the paper evaluates the suitability of the various available beamformers for interference mitigation, considering not only the attenuation provided by them but also their impact on the GNSS UE performance. Finally, since the beamformer performance is bounded to the limitation on the number of antennas, a statistical analysis of the effective Carrier-to-Noise ratio ($C/N_{0_{\text{eff}}}$) with a sweep on the DoA of the interference and the GNSS signal has been performed, along with the case of multiple interferences. These analyses have been performed for five possible antenna array distributions to find the optimal structure for the little available space. Namely, a Uniform Rectangular Array (4-URA) and a Y-shaped array (4-Y) have been considered for the case of four antennas, an L-shaped array (3-L) and an array with its antennas equispaced (3-eq) for three antennas, along with the Uniform Linear Array (2-ULA) for two antennas.

II. Signal Model and Problem Statement

A. Signal Model

Let us consider an array with L antenna elements that receives the superposition of a LOSS of interest with a set of M undesired interferences. The signal perceived by the antennas can be arranged into an $L \times 1$ vector $\mathbf{x}(n)$, thus leading to the following complex basedband signal model at the array output,

$$\mathbf{x}(n) = \alpha_0 \mathbf{a}(\theta_0) s(n) + \sum_{m=1}^{M} \alpha_m \mathbf{a}(\theta_m) i_m(n) + \mathbf{e}(n) \qquad (1)$$

with $s(n)$ the desired signal, $i_m(n)$ the interference/s and $\mathbf{e}(n)$ a vector embedding the noise introduced by each antenna channel. The scalar α denotes a complex amplitude encompassing information about the signal power, with the subscript $_0$ referring to the LOSS and $_m$ to the interference/s. The term $\mathbf{a}(\theta) \in \mathbb{C}^{L\times 1}$ is the spatial signature of the signal coming from direction θ as perceived by the various antennas in the array, and it depends on the antenna inter-separation and the array distribution. In the remainder of the paper, $\mathbf{a}(\theta_0)$ is simply referred to as $\mathbf{a}_0$.

The samples in (1) collected during an observation of interval of N samples can be arranged into the $L \times N$ matrix, $\mathbf{X} \doteq \begin{bmatrix}\mathbf{x}(0) & \mathbf{x}(1) & \dots & \mathbf{x}(N-1)\end{bmatrix}$. The latter will be used in Section III when describing beamforming techniques.

B. The Beamforming Principle

Beamforming is the process of linearly combining the signal samples coming from each of the antennas in the receiver array with the aim of concentrating the array beam towards a specific DoA, while filtering out the contributions coming from other specific DoAs. This can be achieved by applying a set of spatial filtering coefficients or *weights* to the signal in (1) perceived by the array, as shown in equation (2).

$$y(n) = \mathbf{w}^H(n) \cdot \mathbf{x}(n) \qquad (2)$$

where $\mathbf{w}(n) \in \mathbb{C}^{L\times 1}$ is the *weight* vector and $y(n)$ is the signal at the beamformer output. Note that $y(n)$ has a scalar magnitude, and thus can be understood as the output of an equivalent *smart* single antenna. The beamforming problem comes down to determining the coefficients in $\mathbf{w}(n)$ that satisfy a given design criterion, which is where the beamforming techniques come into play, as explained next.

III. Beamforming Techniques for Interference Mitigation

Interference mitigation by means of spatial filtering can be implemented either before or after the de-spreading at the GNSS receiver, what is often known as pre- or post-correlation, respectively. Pre-correlation is adopted herein because it is at this stage, before de-spreading, where interference signals are more visible and can thus be easily detected. Unlike multipath or spoofing, interferences are uncorrelated with the GNSS signal and received with a much larger power, thus greatly simplifying the mitigation process. Following the pre-correlation approach, the beamformers considered herein will therefore work with the samples obtained at the output of the RF front end of the receiver, before the correlation with the local replica. Such beamforming techniques are briefly presented next.

A. Phased Array

The Phased Array beamformer (PA) is certainly the simplest technique. Its underlying idea is to sum the contribution of the signal received at each antenna when the antenna array is pointing at the direction of the LOSS. Accordinly, the PA can only improve the SNR by a factor of $10\log_{10}(L)$ and its weights are given by,

$$\mathbf{w}_{\text{PA}} = \mathbf{a}_0. \qquad (3)$$

This beamformer is thus just a spatial matched filter to the spatial signature of the received signal when the spatial noise is uncorrelated among antenna elements. However simple, its performance is poor for interference mitigation.

B. Capon beamformer

The *Capon* beamformer, also known as the *Minimum Variance Distortionless Response* beamformer (MVDR) is a rather general beamforming approach. The weights of this beamformer come from minimising the power of the received signal subject to a constraint in the DoA of the LOSS, which keeps it from altering the desired signal. The MVDR is capable

of enhancing the SNR by the same factor as the PA, but with the addition of the power minimisation condition,

$$\min_{\mathbf{w}} P_y = \min_{\mathbf{w}} \mathbf{w}^H \mathbf{R}_{\mathbf{x}} \mathbf{w} \text{ subject to } \mathbf{a}_0^H \mathbf{w} = 1 \tag{4}$$

which leads to the weights,

$$\mathbf{w}_{\text{MVDR}} = \frac{\mathbf{R}_{\mathbf{x}}^{-1} \mathbf{a}_0}{\mathbf{a}_0^H \mathbf{R}_{\mathbf{x}}^{-1} \mathbf{a}_0} \tag{5}$$

where $\mathbf{R}_{\mathbf{x}} \doteq \left[\mathbf{X}\mathbf{X}^H\right] \in \mathbb{C}^{L \times L}$ is the auto-correlation matrix of the data in $\mathbf{X}$. Since the MVDR is solely based on power, and at pre-correlation stage the only visible power is that of the interference signal, the MVDR will tend to place nulls in the beampattern at the DoA where intereferences are located.

C. Power Inversion

The main idea of the *Power Inversion* beamformer (PI) is to minimise the total power at the array output under the constraint that one of the antennas (the reference one) must keep its weight equal to 1. In fact, the array architecture can be thought of as the reference antenna plus a set of auxiliary antennas. Effectively, this beamformer chooses the weights pertinent to the auxiliary antennas in such a way that the interference component in the reference antenna is suppressed, which is an approach similar to that of the SideLobe Canceller (SLC) in RADAR applications.
The criterion for the weight calculation is the following,

$$\min_{\mathbf{w}} \mathbf{w}^H \mathbf{R}_{\mathbf{x}} \mathbf{w} \text{ subject to } \boldsymbol{\delta}_1^H \mathbf{w} = 1 \tag{6}$$

which leads to the following weights,

$$\mathbf{w}_{\text{PI}} = \frac{\mathbf{R}_{\mathbf{x}}^{-1} \boldsymbol{\delta}_1}{\boldsymbol{\delta}_1^H \mathbf{R}_{\mathbf{x}}^{-1} \boldsymbol{\delta}_1} \tag{7}$$

where $\boldsymbol{\delta}_1 = [1, 0, ..., 0]$ is the Kronecker delta, the position of the '1' being the position of the reference antenna in the array.

IV. Methodology for Assessing Interference Mitigation Performance in GNSS Receivers

The obtention of the attenuation values provided by the beamformer is clear and has been presented in the literature for a higher amount of antennas. However, while the nulling capability of the beamformer is a good indicator on its performance, more direct and key indicators on performance of a GNSS receiver are the C/N_0 as well as the carrier phase and code jitters.

The general outline for the methodology followed to obtain these parameters is shown in Figure 1. As can be seen on the left hand side of this figure, knowing the Signal-to-Interference ratio (SIR) at the input of the beamformer (that is, knowing the the power ratio between the GNSS signal and the interference), one can then compute the corresponding SIR at the output of the beamformer by knowing the interference cancellation brought by the antenna array, namely β_{DBF}. In this way, $\text{SIR}_{\text{out}}(\text{dB}) = \text{SIR}_{\text{in}}(\text{dB}) + 10\log_{10}\beta_{\text{DBF}}$. Once the SIR at the output of the antenna array is known, the effective C/N_0 that a GNSS receiver will perceive in the presence of the residual interference that might still be present, is given by [17]:

$$(C/N_0)_{\text{eff}} = \left(\frac{1}{(C_s/N_0)} + \sum_{m=1}^{M} \frac{1}{\text{SIR}_{\text{out},m} \cdot Q_m R_c} \right)^{-1} \tag{8}$$

where C_s/N_0 is the nominal C/N_0 (i.e. the C/N_0 when no interferences are present), R_c is the spreading code rate (e.g. 1.023 Mchips/s) and Q is the jamming resistance quality factor [17, Eq. 6.9]. A Continuous Wave (CW) interference has been chosen for our simulations since it is the most degrading case (with a $Q = 1$) [17]. With the effective C/N_0 estimates obtained from (8), the code and phase jitters can be estimated if the parameters of the Delay Lock Loop (DLL) and the Phase Lock Loop (PLL) in the receiver are known, by using [17, Eq. 6.32], where the C/N_0 should be substituted for the $(C/N_0)_{\text{eff}}$, and [17, Eq. 5.7], respectively. Noticeably, [17, Eq. 6.32] shows a dependency on f^2 and on the GNSS signal spectrum at the baseband frequency of the interference, for the delay jitter calculation. This entails that the interference causes higher errors in the DLL if its frequency is higher. Meanwhile, the error in the PLL has the opposite effect, it is higher for lower frequencies. For our simulations we have considered an interference with $f = 0\,Hz$, which is the most damaging for the PLL.

This set of equations provides a relationship between the code and phase jitters, the effective C/N_0 and the SIR at the output of the beamformer. Hence, by knowing only one of these parameters, the others can be estimated. Typically, certain requirements have to be met in the jitters and/or the C/N_0 and therefore, this method provides the attenuation levels that the beamformer needs to provide to reach such requirements.

V. Simulation Results

The results in this Section follow the methodology described in Section IV, abridged in Figure 1. First, the SIR_{in} is deter-

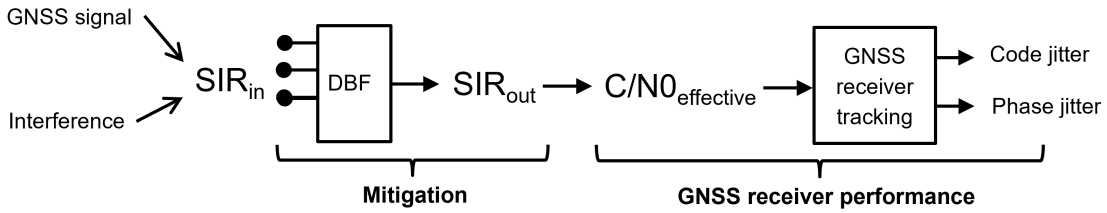

Fig. 1: Block diagram of the methodology

TABLE I: Scenario definition

Scenario	Received interference power (dBW)	**Input SIR (dB)**	Distance between transmitter and receiver (m)		
			0.1 W transmitter	1 W transmitter	4 W transmitter
1) Strong interf.	-55	**-103.5**	3	10	20
2) Weak interf.	-95	**-63.5**	300	1000	2000

mined by defining the scenarios for the interference, in Section V-A. Then, the cancellation of the beamformer is computed, and the effective C/N_0 is obtained with (8). Finally, the effective C/N_0 is compared to a limit C/N_0 given by a set of requirements on the code and phase jitters, in V-B. Following this methodology, the performance of the beamformer will be assessed for different array configurations representative of a GNSS handheld device.

Digital beamforming for handheld devices tends to struggle in distinguishing the LOSS from the interference due to the small array geometry. In contrast, for a high number of antennas, the main lobe has a thin beamwidth, which allows it to be spatially separated from the null placed for the interference. However, reducing the number of antennas enlarges the beamwidth of the main lobe, which affects the cancellation of the interference. In order to shed light onto this effect, a statistical analysis has been carried out for determining the attenuation and effective C/N_0 for a wide sweep of DoAs of LOSS and interference. It is performed for all the proposed antenna array architectures, for the case of one interference in Section V-C, or multiple interferences in Section V-D.

A. Definition of scenarios and operation zone

Coming back to the methodology in Figure 1, the first step is to determine the input SIR to be considered for the scenarios where the interference mitigation performance is to be analysed. The input SIR depends, on the one hand, on the power of the GNSS signals, which is assumed to be -158.5 dBW [18], and, on the other hand, on the power of the interference signal that is received at the GNSS UE. The latter depends in turn, on both the transmit power of the interference source and on the distance from such transmitter to the GNSS UE. Two scenarios will be considered henceforth representing either a strong or a weak interference signal. The representative power levels of these two cases will be assumed to be -55 dBW and -95 dBW, respectively, which correspond to different situations of transmit power and distance, as shown in table I.

The operation range for the interference mitigation techniques to be considered herein is thus defined according to these two scenarios, so that any interference between -95 dBW and -55 dBW is considered to be in the operation zone. These two scenarios are interesting because the beamformer performance strongly varies with the received power of the interference. The resulting SIR_{in} values turn out to be contained within the range of -103.5 dB to -63.5 dB.

Finally, the requirement for our code and phase jitters has been set to 15 cm and 1.4 mm, respectively. Following [17, Eq. 5.7] and [17, Eq. 6.32], the minimum required C/N_0 that needs to be preserved in order to provide the aforementioned jitter, has been found to be 44.2 dBHz, which is the worst case among the two jitter requirements.

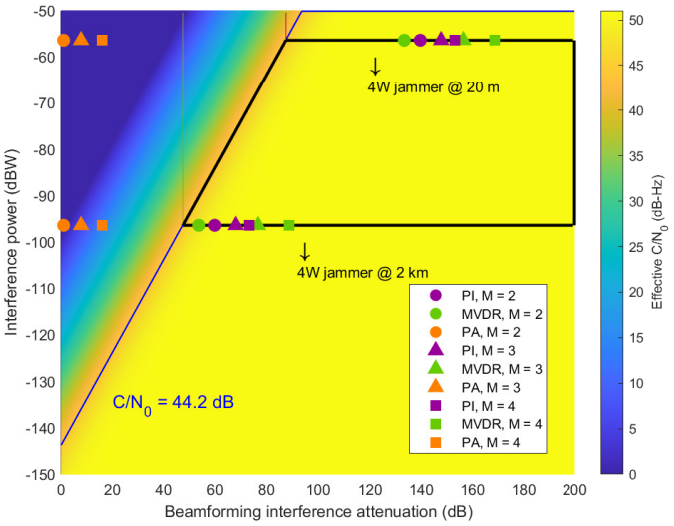

Fig. 2: Effective C/N_0 as a function of interference power and beamforming attenuation using the MVDR, PI or PA for various antenna array structures with *M* antennas

B. Beamformer interference cancellation and corresponding effective C/N0

Once the SIR_{in} is known, the next step is to obtain the SIR_{out} and corresponding effective C/N_0, following Figure 1. In doing so, the PA, PI and MVDR have been tested for a CW interference, although this result can be extrapolated to any type of interference since these algorithms rely on power. Following the definition of each beamformer and (8), the attenuation values and the effective C/N_0 have been obtained, considering the operation range defined in the previous Section.

These values have been printed onto Figure 2, which shows all the parameters at hand: the attenuation levels of each beamformer against interference power, the corresponding effective C/N_0, and a comparison with the values set by a requirement in the code and phase jitters. This figure conveys very nicely all the parameters at hand, and can be easily used as a reference when checking the necessary attenuation given some requirement in the C/N_0. Furthermore, the operation zone is marked by the black trapezoid with a delimitation set by the requirement. Any attenuation value provided by the beamformer inside this trapezoid complies with the requirement.

The two scenarios in Table I have been considered in Figure 2 setting a nominal C/N_0 of 45 dBHz as the representative one for outdoor working conditions. The DoA of the LOSS is equal to $[0°, 0°]$, and that of the interference equal to $[85°, 20°]$ in [elevation, azimuth]. As expected, the results of the PA are the worst, located far away from the trapezoidal region in Figure

2 compliant with the requirements. In contrast, both the PI and MVDR provide good cancellation, although the MVDR presents better results because of the added signal enhancement. Nonetheless, the results clearly show that the higher the interference power, the better the beamformer attenuation and, with it, the effective C/N_0. Since these beamformers are based on power, they struggle with lower-powered interferences, but they excel when the interference can be clearly distinguished in the signal spectrum. Nonetheless, our requirement of having a $C/N_{0_{\text{eff}}}$ above the 44.2 dBHz set by the PLL and DLL jitters is still met in all cases.

C. Statistical analysis: one interference case

This Section presents the results on the attenuation levels and effective C/N_0 achieved by the MVDR beamformer by exhaustively varying the DoA of both the LOSS and the one interference. They have been simulated using the weak interference power in Table I, that is -95 dBW received power, corresponding to the lower line of the trapezoid in Fig. 2 (i.e. 4W transmit power, with a receiver at 2 km). The results for the strong interference case are less interesting because in this case, the beamformer easily identifies the interference and the cancellation is practically always enough to provide the maximal C/N_0 values, as explained in Section V-B.

The results are shown in Fig. 3 by showing the aggregate statistical distribution of the MVDR cancellation when the DOA of the LOSS is placed at $0°$ azimuth and ranges from $0°$ to $90°$ elevation, while the DOA of the interference is placed at $30°$ azimuth and ranges from $0°$ to $60°$ elevation. The X-axis of Fig. 3 represents the MVDR cancellation, where a red line indicates the minimum cancellation that is needed to be compliant with the requirements set in Section V-A (i.e. the lower left hand corner of the trapezoid in Fig. 2).

Figure 3 shows that using four antennas instead of three does not carry a substantial gain, while the gain from two to three is considerable since the 2-ULA does not have spatial diversity in azimuth. Between the three antenna options, the 3-eq is marginally better, while the 4-Y is also somewhat better than the 4-URA (complying with [19], [20]) because the results have less variance and adhere better to the requirement. In this sense, using either of the three antenna options is encouraged due to the increase in complexity of using four antennas. For small handheld devices, these results also show that using two antennas still provides decent performance, as shown in Figure 4. For the case of bigger devices such as tablets, the 4-URA may be preferred over the 4-Y due to it occupying less space, since the separation between antennas for the 4-URA can be $\lambda/2$.

Noticeably, while the effects of the antenna radiation pattern on the interference cancellation are not included in this analysis (they are considered to be zero), the difference in the results will not be high since the quality of the antennas of handheld devices is low and do not provide much attenuation to the interference/s *per se*.

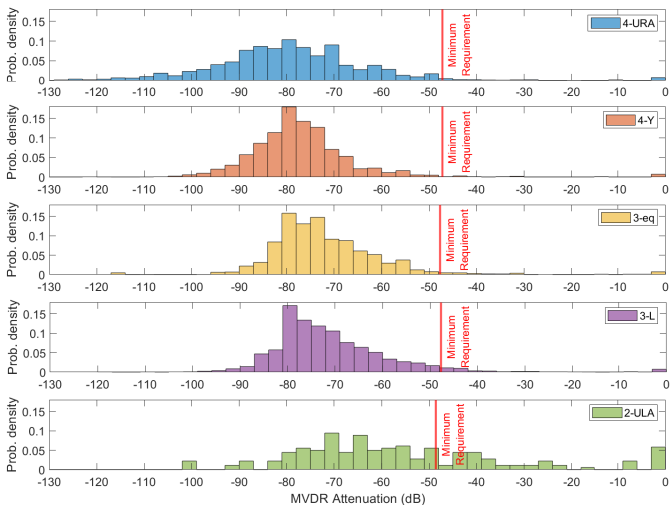

Fig. 3: Histogram of the attenuation provided by each of the proposed antenna arrays with the MVDR beamformer for all possible combinations of DoAs of the LOSS and the interference.

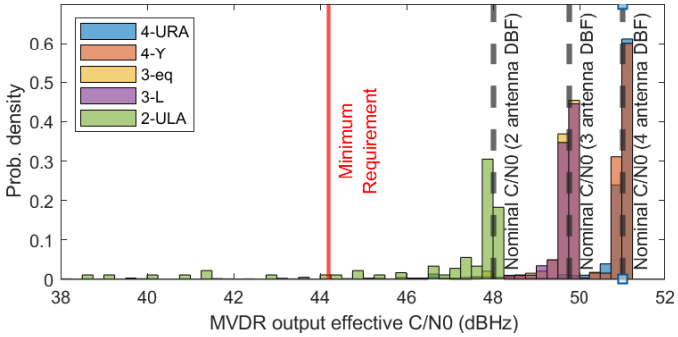

Fig. 4: Histogram of $C/N_{0_{\text{eff}}}$ provided by each antenna array using MVDR.

D. Statistical analysis: two interferences case

This Section considers the same analysis in Section V-C but for the case of two interferences. The second interference has the same DoA range as the first one, as described in Section V-C. The 2-antenna array is not considered since it cannot mitigate more than one interference. Figure 5 shows the attenuation values for each of the proposed antenna arrays in a 3D histogram that combines them. As in the case for one interference, using four antennas does not massively improve performance with respect to using three, although it does so more than the one interference case. As expected, the requirement is tougher to reach with two interferences, but the difference is not massive in comparison with the one-interference case, and the requirement is still met in most DoA combinations.

One special case is when both interferences are very spatially close to the LOSS (that is, for a difference in only elevation or azimuth between $10°$ and $30°$), in which the 4-Y does mitigate the interferences much better than the 4-

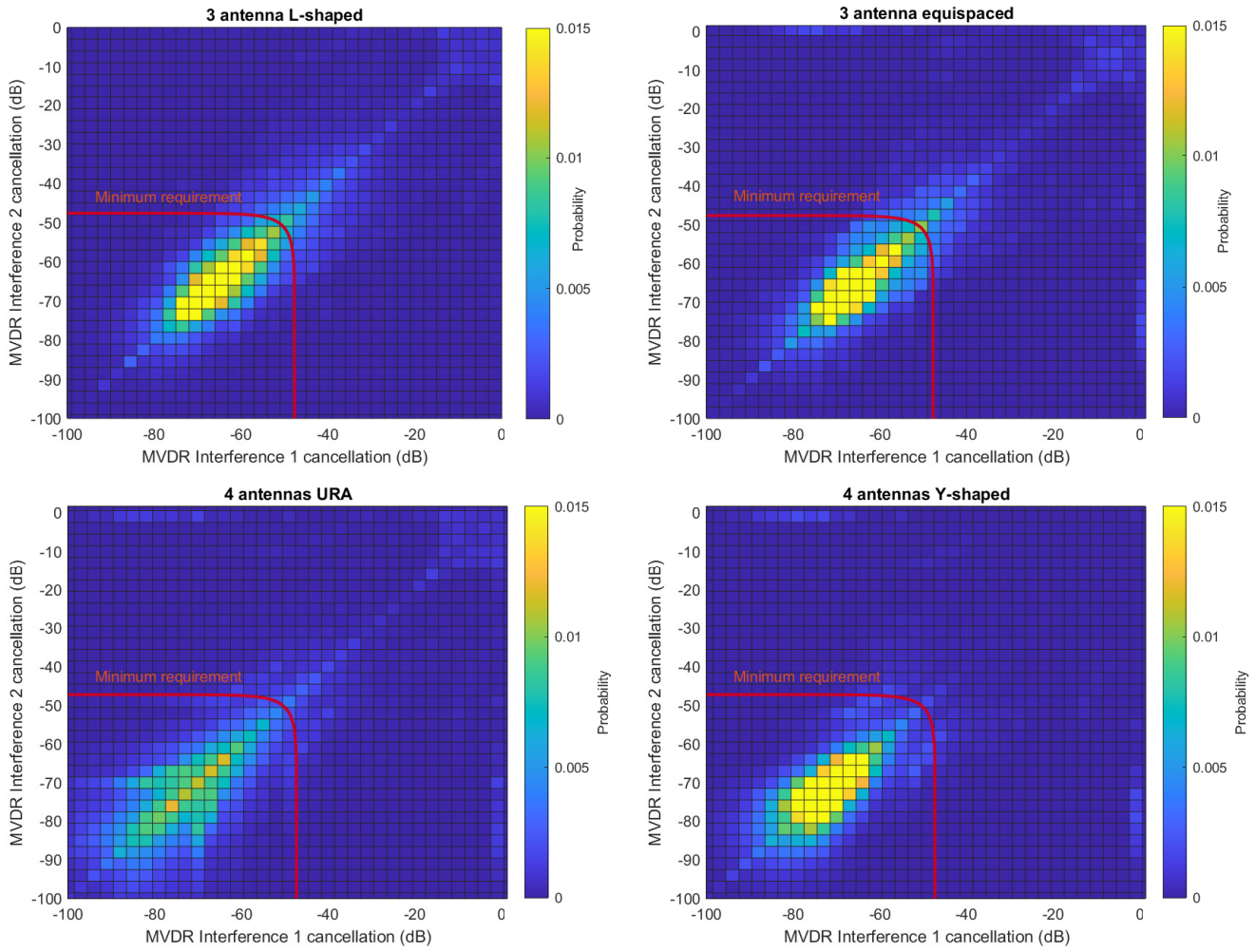

Fig. 5: Top-view of the 3D histogram of the attenuation values for each array architecture.

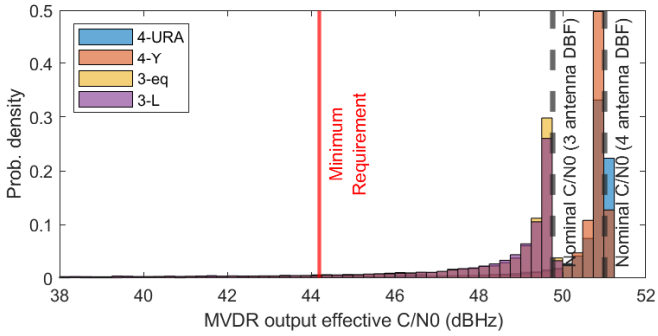

Fig. 6: Histogram of $C/N_{0_{\text{eff}}}$ provided by each antenna array using MVDR, for two interferences.

URA, 3-eq and 3-L, no matter the interference power. While this improvement is very specific, it may be crucial in some applications, although it is not generally impactful. For the vast majority of cases, all considered arrays comply with our requirement, as shown in Figure 6, and the three-antenna array would still trump over the four-antenna options due to decreased space use and complexity.

VI. Conclusion

In this paper we have evaluated the feasibility of performing interference mitigation with beamforming techniques using a small number of antennas. A simulation campaign has been carried out to benchmark various antenna array configurations that can adapt to the small available area of a handheld terminal. The proposed methodology is capable of combining GNSS key performance metrics, such as the effective C/N_0 and code and phase jitters, and relating them with beamforming attenuation. Results show that three-antenna array structures provide the best results in a tradeoff between performance and complexity. When two interferences are present, the four antenna Y-shaped trumps all the other options only if both interferences are very spatially close to the LOSS. Furthermore, although three- or four-antenna arrays provide better performance, decent results are obtained for two-antenna arrays, thus confirming the suitability of the latter for the practical implementation in small devices such as smartphones.

REFERENCES

[1] M. Sahmoudi and M. G. Amin, "Optimal Robust Beamforming for Interference and Multipath Mitigation in GNSS Arrays," in *Proc. of the IEEE International Conference on Acoustics, Speech and Signal Processing (ICASSP)*, vol. 3, 2007, pp. III–693–III–696.

[2] M. L. Psiaki, B. W. OHanlon, S. P. Powell, J. A. Bhatti, K. D. Wesson, and T. E. H. A. Schofield, "GNSS Spoofing Detection Using Two-Antenna Differential Carrier Phase," *Proc. of the International Technical Meeting of the Satellite Division of The Institute of Navigation (ION GNSS+)*, vol. 14, 9 2014.

[3] M. Z. H. Bhuiyan, N. G. Ferrara, S. Thombre, A. Hashemi, M. Pattinson, M. Dumville, M. Alexandersson, E. Axell, P. Eliardsson, M. Pölöskey, V. Manikundalam, S. Lee, and J. R. Gonzalez, "H2020 STRIKE3: Standardization of Interference Threat Monitoring and Receiver Testing - Significant Achievements and Impact," in *Proc. of the European Microwave Conference in Central Europe (EuMCE)*, 2019, pp. 311–314.

[4] A. L. Swindlehurst, B. D. Jeffs, G. Seco-Granados, and J. Li, "Applications of Array Signal Processing," in *Academic Press Library in Signal Processing: Volume 3*, ser. Academic Press Library in Signal Processing, A. M. Zoubir, M. Viberg, R. Chellappa, and S. Theodoridis, Eds. Elsevier, 2014, vol. 3, pp. 859–953.

[5] J. Capon, "High-resolution frequency-wavenumber spectrum analysis," *Proc. IEEE*, vol. 57, no. 8, pp. 1408–1418, 1969.

[6] A. Konovaltsev, F. Antreich, and A. Hornbostel, "Performance assessment of antenna array algorithms for multipath and interferers mitigation," in *Proc. of the Workshop on GNSS Signals & Signal Processing (GNSS SIGNALS)*, April 2007.

[7] R. Compton, "The Power-Inversion Adaptive Array: Concept and Performance," *IEEE Trans. on Aerosp. Electron. Systems*, vol. 15, no. 6, pp. 803–814, 1979.

[8] E. G. Larsson, O. Edfors, F. Tufvesson, and T. L. Marzetta, "Massive MIMO for next generation wireless systems," *IEEE Commun. Mag.*, vol. 52, no. 2, pp. 186–195, 2014.

[9] F. Rusek, D. Persson, B. K. Lau, E. G. Larsson, T. L. Marzetta, O. Edfors, and F. Tufvesson, "Scaling Up MIMO: Opportunities and Challenges with Very Large Arrays," *IEEE Signal Process. Mag.*, vol. 30, no. 1, pp. 40–60, 2013.

[10] F. W. Vook, A. Ghosh, and T. A. Thomas, "MIMO and beamforming solutions for 5G technology," in *2014 IEEE MTT-S International Microwave Symposium (IMS2014)*, 2014, pp. 1–4.

[11] Ö. T. Demir, E. Björnson, L. Sanguinetti *et al.*, "Foundations of user-centric cell-free massive mimo," *Foundations and Trends® in Signal Processing*, vol. 14, no. 3-4, pp. 162–472, 2021.

[12] H. T. Chattha, "4-Port 2-Element MIMO Antenna for 5G Portable Applications," *IEEE Access*, vol. 7, pp. 96 516–96 520, 2019.

[13] N. O. Parchin, Y. I. A. Al-Yasir, A. H. Ali, I. Elfergani, J. M. Noras, J. Rodriguez, and R. A. Abd-Alhameed, "Eight-Element Dual-Polarized MIMO Slot Antenna System for 5G Smartphone Applications," *IEEE Access*, vol. 7, pp. 15 612–15 622, 2019.

[14] A. Ahmad, D.-y. Choi, and S. Ullah, "A compact two elements mimo antenna for 5g communication," *Scientific Reports*, vol. 12, no. 1, p. 3608, 2022.

[15] N. Vagle, A. Broumandan, and G. Lachapelle, "Analysis of Multi-Antenna GNSS Receiver Performance under Jamming Attacks," *Sensors*, vol. 16, no. 11, 2016.

[16] M. Brenneman, J. Morton, C. Yang, and F. van Graas, "Mitigation of GPS Multipath Using Polarization and Spatial Diversities," *Proc. of the Technical Meeting of the Satellite Division of The Institute of Navigation (ION GNSS))*, 2007.

[17] E. Kaplan and C. Hegarty, *Understanding GPS/GNSS: Principles and Applications, 2nd Edition*, 2006.

[18] F. Moorefield, "Global positioning system standard positioning service performance standard 5th edn," 2020.

[19] M. Martín-Neira and J. M. Goutoule, "MIRAS- A two-dimensional aperture-synthesis radiometer for soil-moisture and ocean-salinity observations," *ESA bulletin*, no. 92, pp. 95–104, 1997.

[20] P. Silvestrin, M. Berger, Y. Kerr, and J. Font, "ESA's second earth explorer opportunity mission: The soil moisture and ocean salinity mission—SMOS," *IEEE Geosci. Remote Sens. Newslett*, vol. 118, pp. 11–14, 2001.